0351

INCORPORATION OF THE EFFECT OF BIAXIAL STRESSES IN THE AVERAGE STRES-STRAIN RELATIONSHIP OF REBAR IN RC PANELS

Amlan K SENGUPTA[1] And Abdeldjelil BELARBI[2]

SUMMARY

The load versus deformation behavior of a reinforced concrete (RC) panel element under membrane stresses can be predicted by the modified compression field theory (MCFT) and the softened truss model (STM). In these theories, the stress–strain relationships for reinforcing bars are derived from tests with uniaxial tension. When these relationships are applied to an element under biaxial stresses, the Poisson's effect is neglected. This leads to an unconservative overestimate of the shear resistance offered by the element. The present research investigated the Poisson's effect in RC panels and refined the existing formulation of the STM. To incorporate the Poisson's effect in the analysis of panels, an orthotropic formulation was developed, based on the concept of apparent Poisson's ratio (APR). The APRs were quantified by testing panels under biaxial tension–compression. It was demonstrated that when the Poisson's effect is incorporated, the predicted behavior of a panel gets closer to the experimental results.

INTRODUCTION

Wall– and shell–type structures, like shear walls, nuclear containment vessels and beams with deep and thin webs, are common applications of reinforced concrete (RC). The predominant stresses in the walls of these structures are two dimensional in-plane normal and shear stresses, which are commonly referred to as membrane stresses. The analysis of these structures can be performed by the finite element method, where the wall is usually visualized as an assemblage of rectangular elements. A rectangular element subjected to membrane stresses, is referred to as a "panel element". The two elegant theories for predicting the load–deformation behavior of a panel element, are the modified compression field theory (MCFT) [Vecchio and Collins, 1986] and the softened truss model (STM) [Hsu, 1993]. The two theories are based on the equilibrium of external and internal stresses, the compatibility of strains in concrete and reinforcing bars (rebar) and the constitutive relationships of concrete and rebar. The stress–strain relationships of rebar under tension are based on tests of bare rebar, with the assumption of elastic–perfectly-plastic behavior (as in the MCFT), or are derived from tests of panels with a state of uniaxial stress (as in the STM, Belarbi and Hsu, 1994). The relationships are applied, without any modification, to panel elements under a state of biaxial stresses generated from shear. This leads to an anomaly in the predicted behavior of a panel element. In order to rectify the drawback, the present research investigates the effect of biaxial stresses in the constitutive relationship of rebar. Rectification of the anomaly leads to the prediction of a realistic shear resistance of a panel element, with reduced capacity at ultimate load and increased deformation at service load. This is encouraging as regards the prediction of ductility and the design of reinforcement in wall– and shell–type structures located in earthquake prone areas.

SOFTENED TRUSS MODEL

The present formulation of the effect of biaxial stresses is based on the STM and hence, a brief introduction of the STM

is provided. The STM was developed at University of Houston for predicting the postcracking nonlinear behavior of RC panel elements under membrane stresses. An important aspect of the STM is the concept of 'average' stresses and 'average' strains. After cracking, although the concrete becomes discontinuous, the

[1] *Ove Arup & Partners California, Los Angeles, California, USA, Email: amlan.sengupta@arup.com*
[2] *Department of Civil Engineering, University of Missouri–Rolla, Rolla, Missouri, USA, Email: belarbi@umr.edu*

reinforced concrete is treated as a continuous homogenous medium, with the values of stresses and strains as average quantities along the finite dimensions of an element. Henceforth, the terms stress and strain will be used to refer to the average values, unless mentioned otherwise.

Three coordinate systems are defined to express the equations of equilibrium and compatibility, and the constitutive relationships. First, the longitudinal (ℓ) and transverse (t) directions of the orthogonal grid of reinforcement constitute the ℓ–t coordinate system (Fig. 1). The applied external normal (σ_ℓ and σ_t) and shear stresses ($\tau_{\ell t}$) are expressed in this coordinate system. Second, when the external stresses are expressed in terms of the principal stresses (σ_2 and σ_1), the directions of the principal stresses constitute the 2–1 coordinate system. σ_2 and σ_1 represent the compressive stress and tensile stress, respectively, for elements under predominant shear stresses. The third coordinate system is related with the internal stresses in concrete. When the stresses in concrete are expressed in terms of the principal compressive stress (σ_d) and the principal tensile stress (σ_r), the directions of the two principal stresses constitute the d–r coordinate system. The inclinations of the 2–1 and the d–r coordinate systems with respect to the ℓ–t coordinate system are denoted as α_2 and α, respectively.

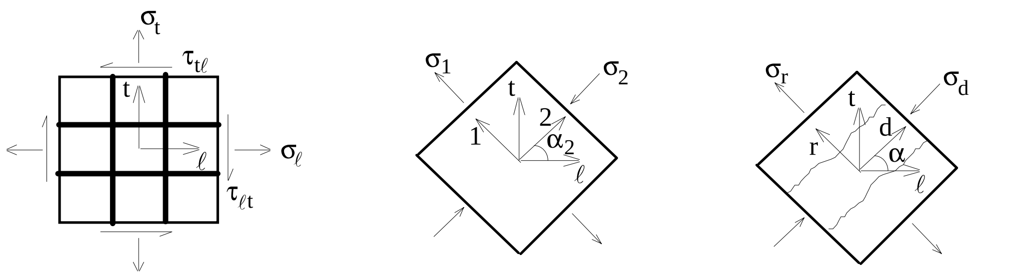

a) Applied stresses

b) Principal axes 2 and 1 for applied stresses

c) Principal axes d and r for stresses in concrete

Figure 1. Coordinate systems in panel element

The equations of equilibrium and compatibility, and the constitutive relationships of the STM are as follows.

Equations of equilibrium

$$\begin{aligned} \sigma_\ell &= \sigma_d \cos^2\alpha + \sigma_r \sin^2\alpha + \rho_\ell f_\ell \\ \sigma_t &= \sigma_d \sin^2\alpha + \sigma_r \cos^2\alpha + \rho_t f_t \\ \tau_{\ell t} &= (-\sigma_d + \sigma_r)\sin\alpha\cos\alpha \end{aligned} \qquad \textbf{(1)}$$

Here, ρ_ℓ and ρ_t are the reinforcement ratios along ℓ- and t- axes, respectively. The corresponding stresses in the rebar are f_ℓ and f_t, respectively. It is assumed that the rebar carries axial stresses only, that is, the dowel action is neglected.

Equations of compatibility

$$\begin{aligned} \varepsilon_\ell &= \varepsilon_d \cos^2\alpha + \varepsilon_r \sin^2\alpha \\ \varepsilon_t &= \varepsilon_d \sin^2\alpha + \varepsilon_r \cos^2\alpha \\ \gamma_{\ell t} &= 2(-\varepsilon_d + \varepsilon_r)\sin\alpha\cos\alpha \end{aligned} \qquad \textbf{(2)}$$

Here, ε_ℓ and ε_t are the normal strains and $\gamma_{\ell t}$ is the shear strain in the ℓ–t coordinate system. Assuming the principal axes to be same for the stress and strain, the principal strains in concrete along d- and r- axes are denoted as ε_d and ε_r, respectively.

Constitutive relationships

Concrete in compression

For the ascending branch ($\varepsilon_d/\zeta\varepsilon_0 \le 1$), the parabolic relationship is as follows.

$$\sigma_d = \zeta f_c^/ [2(\frac{\varepsilon_d}{\zeta \varepsilon_0}) - (\frac{\varepsilon_d}{\zeta \varepsilon_0})^2] \quad \textbf{(3)}$$

The cylinder compressive strength and the strain corresponding to the peak stress in cylinder are denoted as $f_c^/$ and ε_0, respectively. The reductions of the peak compressive stress and the corresponding strain under tensile strain in the perpendicular direction are quantified by the softening coefficient ζ [Belarbi and Hsu, 1995]. The descending branch can be also modeled by a parabolic expression.

Concrete in tension

The average principal tensile stress (σ_r) increases linearly with respect to the average principal tensile strain (ε_r), till cracking. The stiffness is comparable to that for plain concrete. After cracking, σ_r reduces rapidly with increasing ε_r.

Rebar in tension

The bilinear model, developed by Belarbi and Hsu [1994], is provided below. The two equations correspond to the elastic and postelastic stages, respectively.

For $\varepsilon_s \le \varepsilon_n^*$

$$f_s = E_s \varepsilon_s \quad \textbf{(4)}$$

For $\varepsilon_s > \varepsilon_n^*$

$$f_s = f_0^* + E_p^* \varepsilon_s \quad \textbf{(5)}$$

where, f_s or ε_s are the stress and strain in the rebar, respectively. The subscript s is a generalized notation for ℓ and t. E_s is the modulus of steel. The intercept and slope of the postyield curve are denoted as f_0^* and E_p^*, respectively. The strain ε_n^* approximates the apparent yield strain ε_y^*. The apparent yield strain is the strain, beyond which the average stress–strain relationship deviates from the elastic behavior. The stress corresponding to ε_y^* is termed as the apparent yield stress and is denoted as f_y^*. Since the model was developed by testing panels under uniaxial tension, it can be termed as the uniaxial constitutive relationship.

MODELING OF THE EFFECT OF BIAXIAL STRESSES

The drawback in the STM arises due to the neglect of the Poisson's effect in a panel element under biaxial stresses. In a state of biaxial stresses a strain has two components, one caused by the stress along its direction and the other caused by the stress along the perpendicular direction. The two components can be termed as the uniaxial and biaxial components, respectively. The generation of the biaxial component is called the Poisson's effect. In the STM, the two components of the strain are not treated separately. The stress in rebar is related to the total strain by the uniaxial relationship (Eqs. 4 and 5). This leads to overestimates of the rebar stress and consequently the shear stress ($\tau_{\ell t}$) carried by the panel element. As a corollary, the shear deformation ($\gamma_{\ell t}$) is underestimated. Moreover, the theoretical $\tau_{\ell t}$ versus $\gamma_{\ell t}$ curve shows reduction in $\gamma_{\ell t}$ with decreasing $\tau_{\ell t}$ beyond the peak stress in concrete. This contradicts the experimentally observed increasing $\gamma_{\ell t}$. The anomaly arises while maintaining equilibrium between decreasing compressive stress in concrete (σ_d) and increasing tensile stress in the rebar (f_s) due to strain hardening.

The Poisson's effect is direction dependent for anisotropic materials. To quantify the anisotropy with a limited number of variables, the present formulation of the Poisson's effect is limited to orthotropic panel elements with reinforcement symmetric about the principal axes of applied stresses (2–1 coordinate system). In such elements, the d- and r- axes become the axes of symmetry and they are selected to quantify the orthotropy.

To decompose a strain into the uniaxial and biaxial components, the concept of Apparent Poisson's Ratio (APR) was introduced [Belarbi and Sengupta, 1996]. An APR is defined as the negative of the ratio of the biaxial component of the strain in one direction to the uniaxial component of the strain in the perpendicular direction. The strains ε_d and ε_r are each decomposed into the two components as shown below, where the subscripts u and b refer to the uniaxial and biaxial components, respectively. ν^*_{rd} and ν^*_{dr}

are the APRs defined in the d–r coordinate system. They express the effect of tension on the compressive strain and the effect of compression on the tensile strain, respectively. [N] is the matrix containing the APRs.

$$\begin{bmatrix} \varepsilon_d \\ \varepsilon_r \end{bmatrix} = \begin{bmatrix} \varepsilon_{du} + \varepsilon_{db} \\ \varepsilon_{rb} + \varepsilon_{ru} \end{bmatrix} = \begin{bmatrix} 1 & -\nu^*_{rd} \\ -\nu^*_{dr} & 1 \end{bmatrix} \begin{bmatrix} \varepsilon_{du} \\ \varepsilon_{ru} \end{bmatrix} = [N] \begin{bmatrix} \varepsilon_{du} \\ \varepsilon_{ru} \end{bmatrix} \tag{6}$$

According to the above definition, the following are the expressions of the APRs in terms of the strain components.

$$\nu^*_{rd} = -\frac{\varepsilon_{db}}{\varepsilon_{ru}}, \; \nu^*_{dr} = -\frac{\varepsilon_{rb}}{\varepsilon_{du}} \tag{7}$$

The uniaxial components of the rebar strains, $\varepsilon_{\ell u}$ and ε_{tu}, can be expressed in terms of ε_d and ε_r by a strain transformation and in conjunction with Eq. (6) as follows.

$$\begin{bmatrix} \varepsilon_{\ell u} \\ \varepsilon_{tu} \end{bmatrix} = \begin{bmatrix} \cos^2\alpha & \sin^2\alpha \\ \sin^2\alpha & \cos^2\alpha \end{bmatrix} \begin{bmatrix} \varepsilon_{du} \\ \varepsilon_{ru} \end{bmatrix} = [T] \begin{bmatrix} \varepsilon_{du} \\ \varepsilon_{ru} \end{bmatrix} = [T][N]^{-1} \begin{bmatrix} \varepsilon_d \\ \varepsilon_r \end{bmatrix} \tag{8}$$

[T] is the transformation matrix relating the strains in the d–r coordinate system with the strains in the ℓ–t coordinate system. Substituting the expression of $[N]^{-1}$, $\varepsilon_{\ell u}$ and ε_{tu} are as given below.

$$\begin{bmatrix} \varepsilon_{\ell u} \\ \varepsilon_{tu} \end{bmatrix} = \frac{1}{(1-\nu^*_{dr}\nu^*_{rd})} \left(\begin{bmatrix} \varepsilon_\ell \\ \varepsilon_t \end{bmatrix} + [T] \begin{bmatrix} \nu^*_{rd}\varepsilon_r \\ \nu^*_{dr}\varepsilon_d \end{bmatrix} \right) \tag{9}$$

It was found from test results that after cracking, ν^*_{rd} becomes negligible as compared to ν^*_{dr} and its value approaches zero. If ν^*_{rd} is assumed to be zero, Eq. (9) is simplified. A general expression of $\varepsilon_{\ell u}$ and ε_{tu} can be written in the following form.

$$\varepsilon_{su} = \varepsilon_s + f(\alpha)\nu^*_{dr}\varepsilon_d \tag{10}$$

where, $f(\alpha)$ is equal to $\sin^2\alpha$ or $\cos^2\alpha$ for rebar along ℓ- and t- axes, respectively.

The stress f_s can be computed from ε_{su} by the uniaxial relationship. For piecewise linear equations of the uniaxial relationship, as in Eqs. (4) and (5), f_s can be expressed as follows.

$$\begin{aligned} f_s &= F_U(\varepsilon_{su}) = F_U(\varepsilon_s) + f(\alpha)\nu^*_{dr}F_U(\varepsilon_d) \\ &= F_B(\varepsilon_s, \varepsilon_d) \end{aligned} \tag{11}$$

Here, the function F_U represents the uniaxial relationship. The function F_B expresses f_s in terms of the total strains ε_s and ε_d. This function can be termed as the biaxial constitutive relationship of the rebar. The Poisson's effect is incorporated through the term $f(\alpha)\,\nu^*_{dr}\,F_U(\varepsilon_d)$, and this differentiates the biaxial relationship form the uniaxial counterpart. Since ε_d is negative, the term implies a reduction of the stress from the value given by the uniaxial relationship. As a corollary, for a given value of f_s, the corresponding strain by the biaxial relationship is more than the uniaxial relationship. When the curves of the biaxial and uniaxial relationships are overlapped, the biaxial curve appears to be stretched from the uniaxial curve along the strain axis (Fig. 2).

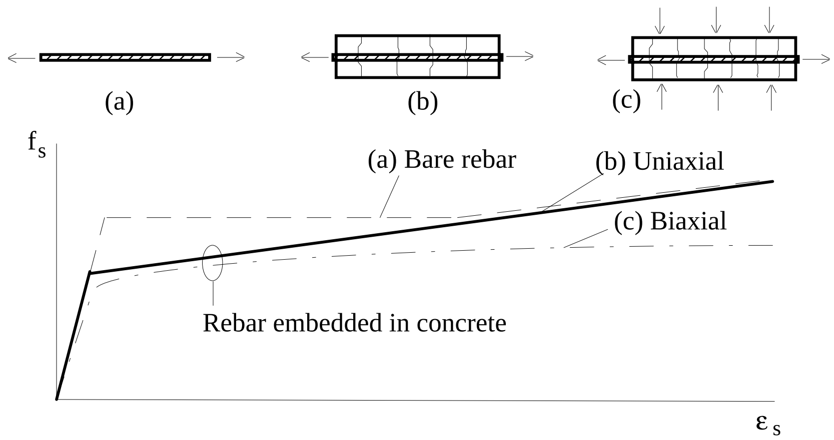

Figure 2. Tensile stress-strain curves for bare rebar and rebar embedded in concrete

A theoretical study was undertaken [Sengupta, 1998] to investigate the Poisson's effect in the panels tested at University of Houston under biaxial tension–compression. It was observed that the APRs do not remain constant throughout the loading history. The value of ν^*_{dr} is high for severely cracked panels and becomes large due to the discontinuity in the medium. It exceeds 0.5, which is the limiting value of Poisson's ratio for a continuous elastic medium. The compressive stress in concrete (σ_d), the tensile stress in the primary longitudinal reinforcement (f_ℓ) and the amount of longitudinal reinforcement (expressed in terms of ρ_ℓ) were identified as parameters that may effect the variation of ν^*_{dr}. On the contrary, ν^*_{rd} was found to decrease rapidly after cracking of concrete.

EXPERIMENTAL RESULTS

The objective of the tests was to measure ν^*_{dr} for panels under biaxial tension–compression and to quantify its variation with respect to the identified parameters σ_d, f_ℓ and ρ_ℓ. The modeling of ν^*_{dr} involves the modeling of ε_{rb} and ε_{du} (Eq. 7). With $\nu^*_{rd} = 0$ after cracking, the expression of ε_{du} is same as that of ε_d, which is available from the constitutive relationship of concrete under compression (Eq. 3). Hence, emphasis was laid on the evaluation of the variation of ε_{rb}. It was also intended to study the effect of the load path on ν^*_{dr} and to confirm the reduction of ν^*_{rd} after the cracking of concrete.

To have parameters comparable for different panels, σ_d and f_ℓ are normalized as $S(\sigma_d) = \sigma_d/\zeta f'_c$ and $R(f_\ell) = f_\ell/f^*_y$, respectively. The factor $\zeta f'_c$ is the instantaneous capacity of concrete in the panel. For rebar, the significance of normalizing f_ℓ with respect to f^*_y is to treat the elastic and postelastic regions separately.

A total of 18 panels were tested in the present program, under biaxial tension–compression [Sengupta, 1998]. The primary longitudinal rebar was aligned along the direction of tension, which implies compression was perpendicular to the ℓ-axis ($\alpha_2 = 90°$). The purpose of selecting this alignment was to quantify the Poisson's effect without the influence of the dowel action in the rebar. The panels were either square (30 in. × 30 in. × 3 in.) or rectangular (42 in. × 30 in. × 3 in.) (1 in. = 2.54 cm). The rectangular panels had additional longitudinal rebar outside the test region, so that yielding occurred in the test region prior to that at the loaded edges.

The panels were subjected to two types of load path. Since the measurement of the APRs imply measurement of the uniaxial and biaxial components of the strains ε_d and ε_r, the load paths were selected such that the strains could be decomposed into the two components correctly and conveniently. The first type was the sequential tension–compression and the second type was the proportional load path, discretized to a stepped scheme.

The 18 panels were divided into 6 series (Table 1). Here, $f_{y\ell}$ and f_{yt} are the yield stresses of the rebar (under bare condition) along ℓ- and t- axes, respectively. The value of $R(f_\ell)$ for a panel correspond to the final tension applied. The panels of each of A-, C- and E- series had identical reinforcement, but they were subjected to different values of $R(f_\ell)$ to study the effect of f_ℓ on the magnitude of ε_{rb}. Panels A1 and C1 were subjected to uniaxial compression ($R(f_\ell) = 0$). For Panels E2 and E3, there was substantial yielding of the rebar. The 4 panels of B-series (including Panel A3, which is also denoted as B2) had varying amount of longitudinal reinforcement, to study the effect of ρ_ℓ. Panel D3 was loaded proportionally till the tension reached a certain value. After that, the tension was kept constant and compression was increased till failure, analogous to sequential loading.

Table 1: Test panel data

Panel	Shape	ρ_ℓ (%)	ρ_t (%)	$f_{y\ell}$ (ksi)†	f_{yt} (ksi)	$f_c^{\prime}$ (psi)	Load path‡	$R(f_\ell)$	Parameters studied
A1	Sq.	0.89	0.49	52.6	54.4	4409	S	0.00	σ_d and f_ℓ
A2	Sq.	0.89	0.49	52.6	54.4	4409	S	0.87	
A3 (B2)	Sq.	0.89	0.49	52.6	54.4	4409	S	0.92	
B1	Sq.	0.44	0.49	52.6	54.4	4409	S	1.02	σ_d and ρ_ℓ
B3	Sq.	1.55	0.49	52.6	54.4	4409	S	0.42	
B4	Sq.	2.00	0.49	52.6	54.4	4409	S	0.57	
C1	Sq.	1.10	0.49	53.8	56.2	5491	S	0.00	σ_d and f_ℓ
C2	Sq.	1.10	0.49	53.8	56.2	5491	S	0.76	
D1	Sq.	1.10	0.49	53.8	56.2	5491	P	0.24	Load path and f_ℓ
D2	Sq.	1.10	0.49	53.8	56.2	5635	P	0.64	
D3	Sq.	1.10	0.49	53.8	56.2	5635	P-S	0.68	
D4	Sq.	1.10	0.49	53.8	56.2	5635	P	0.36	
E1	Rect.	0.86	0.52	56.2	56.2	2701	S	1.01	σ_d and f_ℓ
E2	Rect.	0.86	0.52	56.2	56.2	2825	S	1.13	
E3	Rect.	0.86	0.52	56.2	56.2	3414	S	1.29	
E4	Rect.	0.86	0.52	56.2	56.2	3842	S	0.92	
F1	Rect.	0.86	0.52	56.2	56.2	2763	P	0.80	Load path and f_ℓ
F2	Rect.	0.86	0.52	56.2	56.2	3414	P	1.03	

† 1 ksi = 1000 psi = 6.896 MPa

‡ S: sequential, P: proportional

The variations of ε_{rb} and ν^*_{dr} in absence of tension ($R(f_\ell) = 0$), was studied from Panels A1 and C1. For the rest 16 panels with $R(f_\ell) > 0$, the values of ε_{rb} and ν^*_{dr} were substantially higher. It proved that f_ℓ has a definite influence on the biaxial expansion of a panel. From the B-series panels (panels with varying ρ_ℓ), the effect of ρ_ℓ was not evident. For the panels subjected to sequential loading, although ε_{rb} increased, ν^*_{dr} decreased with increasing σ_d. At the onset of compression, ε_{rb} increased at a higher rate than ε_{du} and hence, large values of ν^*_{dr} were recorded. With increasing compression, the rate of increase of ε_{du} got larger, which resulted in diminishing values of ν^*_{dr}. For panels tested under proportional loading, ν^*_{dr} increased with increasing σ_d. This was because, initially the rate of increase of ε_{rb} was low; but with increasing f_ℓ, the rate got larger. The effect of load path thus originates from the influence of f_ℓ on the increase of ε_{rb}. It was also verified that ν^*_{rd} reduces to zero after cracking.

Modeling of ν^*_{dr}

To model ν^*_{dr}, the expansive strain ε_{rb} is decomposed into two components.

$$\varepsilon_{rb} = \varepsilon^0_{rb} + \varepsilon^{f\ell}_{rb} \tag{12}$$

where, ε^0_{rb} is the strain that would occur under uniaxial compression (that is, in absence of f_ℓ), and $\varepsilon^{f\ell}_{rb}$ is the additional strain in the presence of f_ℓ. From Eq. (7), ν^*_{dr} can be expressed as follows.

$$\nu^{*}_{dr} = -\frac{\varepsilon_{rb}}{\varepsilon_{du}} = \nu^{*0}_{dr} - \frac{\varepsilon^{f\ell}_{rb}}{\varepsilon_{du}} \quad \textbf{(13)}$$

where $\nu^{*0}_{dr} = -\varepsilon^{0}_{rb}/\varepsilon_{du}$. The modeling of ν^{*}_{dr} involves the modeling of ν^{*0}_{dr}, $\varepsilon^{f\ell}_{rb}$ and ε_{du}. As for ε_{du}, its difference with ε_{d} is negligible (as evident from $\nu^{*}_{rd} = 0$). Hence, the expression of ε_{d} from the stress–strain relationship of concrete under compression can be substituted as the expression of ε_{du}. For $S(\sigma_d) \leq 1$, transposing the terms of Eq. 3,

$$\varepsilon_{du} = \varepsilon_{d} = \zeta\,\varepsilon_{0}[1 - \sqrt{1 - S(\sigma_{d})}] \quad \textbf{(14)}$$

From the panels tested under uniaxial compression, the variation of ν^{*0}_{dr} with respect to $S(\sigma_d)$ is modeled as follows.

$$\nu^{*0}_{dr} = 0.06 + 0.18\,S(\sigma_{d}) \quad \textbf{(15)}$$

Regarding $\varepsilon^{f\ell}_{rb}$, the variation is different before and after the yielding of the rebar. Till yielding, that is with $R(f_\ell) \leq 1$, the variation of $\varepsilon^{f\ell}_{rb}$ is reasonably linear with respect to $R(f_\ell)$ and $S(\sigma_d)$.

For $R(f_\ell) \leq 1$

$$\varepsilon^{f\ell}_{rb} = 0.002\,R(f_{\ell})\,S(\sigma_{d}) \quad \textbf{(16)}$$

At the yielding of the rebar, the variation of $\varepsilon^{f\ell}_{rb}$ with respect to $R(f_\ell)$ has a noticeable jump. Beyond yielding, the variation is again practically linear. In the postyield region, the variation of $\varepsilon^{f\ell}_{rb}$ with respect to $S(\sigma_d)$ is linear up to around $S(\sigma_d) = 0.75$. Beyond that it increases at a higher rate. Based on these observations, the following equation is proposed for the postyield variation of $\varepsilon^{f\ell}_{rb}$.

For $R(f_\ell) > 1$

$$\begin{aligned} \varepsilon^{f\ell}_{rb} &= [0.024\,R(f_{\ell}) - 0.020][0.5\,S(\sigma_{d})] && S(\sigma_{d}) \leq 0.75 \\ &= [0.024\,R(f_{\ell}) - 0.020][0.5\,S(\sigma_{d}) + 17\,(S(\sigma_{d}) - 0.75)^{2.6}] && S(\sigma_{d}) > 0.75 \end{aligned} \quad \textbf{(17)}$$

The models of ν^{*0}_{dr}, $\varepsilon^{f\ell}_{rb}$ and ε_{du} are valid up to the peak compressive stress in concrete ($S(\sigma_d) = 1$). With strain controlled tests, the models of the three quantities and consequently that of ν^{*}_{dr} can be extended beyond the peak stress in concrete.

APPLICATION OF THE MODEL

The STM algorithm developed by Hsu [1993] was modified to incorporate the Poisson's effect [Sengupta, 1998]. Using the algorithm, the shear stress–strain ($\tau_{\ell t}$ versus $\gamma_{\ell t}$) behaviors of selected RC panels tested at University of Houston [Pang and Hsu, 1995] and University of Toronto [Vecchio and Collins, 1986] were predicted and compared with the experimental data. The panels had equal amount of longitudinal and transverse reinforcements with $\alpha_2 = 45°$, and were tested under pure shear. The formulation of the Poisson's effect is applicable for such panels. But in the present experimental program, to avoid the effect of dowel action, panels with $\alpha_2 = 90°$ were tested to quantify ν^{*}_{dr}. Since the expression of ν^{*}_{dr} may not be precise, the results should be viewed as qualitative. As typical examples, Figure 3 shows the $\tau_{\ell t}$ versus $\gamma_{\ell t}$ curves for Panel A2 (tested at University of Houston) and Panel PV8 (tested at University of Toronto), calculated by neglecting and including the APR. It can be noted that the curves including the APR, predict the behavior closer to the experimental values. It is also demonstrated that by extending the model of ν^{*}_{dr} hypothetically beyond the peak stress in concrete, the STM can indeed predict the descending branch of the $\tau_{\ell t}$ versus $\gamma_{\ell t}$ curve when the Poisson's effect is incorporated.

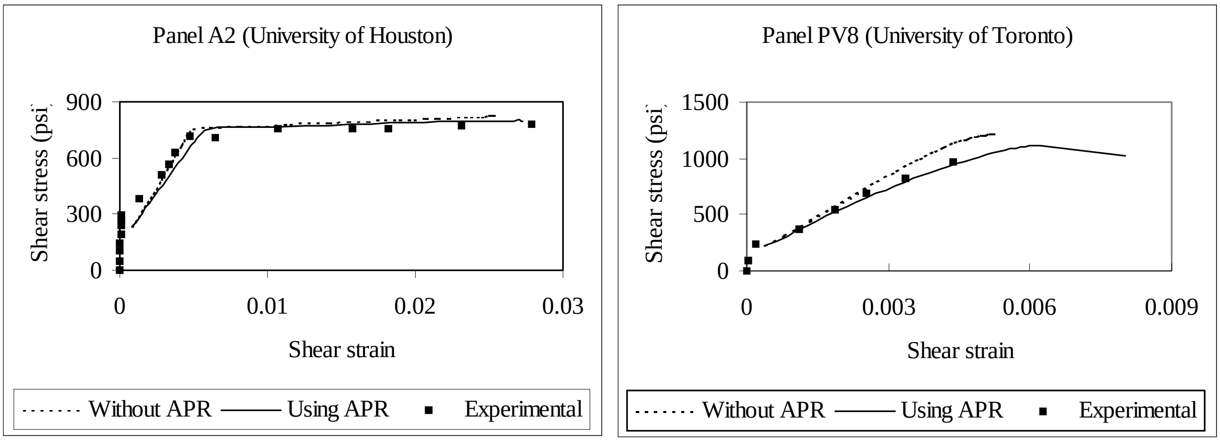

Figure 3. Experimental and predicted shear stress–strain curves

CONCLUSION

The use of the uniaxial stress–strain relationship for rebar under tension in panel elements, leads to an unconservative overestimate of the shear resistance. In the present research, the Poisson's effect is incorporated through the development of the biaxial constitutive relationship for rebar under tension. The concept of apparent Poisson's ratio (APR) is introduced for quantifying the Poisson's effect. Based on the tests of 18 panels, models of the APR are developed. It is shown that with the inclusion of the Poisson's effect, the predicted behavior correlate better with the experimental results. The incorporation of the biaxial effect indeed enhances the capability of the STM in predicting the behavior of panel elements under membrane stresses.

REFERENCES

1. Belarbi, A. and Hsu, T.T.C. (1994), "Constitutive Laws of Concrete in Tension and Reinforcing Bars Stiffened by Concrete," *Structural Journal*, American Concrete Institute, Vol. 91, No. 4, July–August, pp. 465–474.
2. Belarbi, A. and Hsu, T.T.C. (1995), "Constitutive Laws of Softened Concrete in Biaxial Tension–Compression," *Structural Journal*, American Concrete Institute, Vol. 92, No. 5, September–October, pp. 561–573.
3. Belarbi, A. and Sengupta, A.K. (1996), "Average Stress–Strain Relationships of Rebars in RC Panels," *Proceedings* (Edited by Y.K. Lin and T.C. Su), Eleventh Engineering Mechanics Conference, American Society of Civil Engineers, Fort Lauderdale, Florida, May, pp. 743–746.
4. Hsu, T.T.C. (1993), *Unified Theory of Reinforced Concrete*, CRC Press, Florida, 313 pp.
5. Pang, X-B.D. and Hsu, T.T.C. (1995), "Behavior of Reinforced Concrete Membrane Elements in Shear," *Structural Journal*, American Concrete Institute, Vol. 92, No. 6, November–December, pp. 665–679.
6. Sengupta, A.K. (1998), "Average Stress–Strain Relationships of Reinforcing Bars in Concrete Panels Incorporating The Biaxial Stress Field Effect," Ph.D. Dissertation, Dept. of Civil Engg., University of Missouri–Rolla, 310 pp.
7. Vecchio, F.J. and Collins, M.P. (1986), "The Modified Compression–Field Theory for Reinforced Concrete Elements Subjected to Shear," *ACI Journal*, American Concrete Institute, Vol. 83, No. 2, March–April, pp.219–231